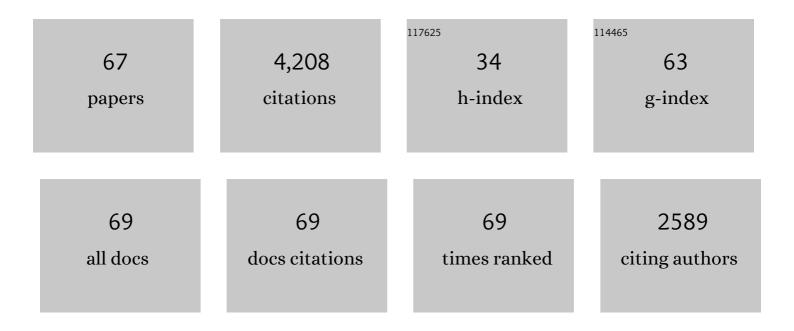
List of Publications by Year in descending order

Source: https://exaly.com/author-pdf/1731043/publications.pdf Version: 2024-02-01



Honeluo

#	Article	IF	CITATIONS
1	Effect of annealing temperatures on microstructural evolution and corrosion behavior of Ti-Mo titanium alloy in hydrochloric acid. Corrosion Science, 2022, 197, 110079.	6.6	30
2	Hydrogen embrittlement of high-strength marine steel as a weld joint in artificial seawater under cathodic polarization. Engineering Failure Analysis, 2022, 134, 106044.	4.0	10
3	Deformation mechanisms of TRIP–TWIP medium-entropy alloys via molecular dynamics simulations. International Journal of Mechanical Sciences, 2022, 219, 107098.	6.7	27
4	Effect of electrochemical hydrogen charging on the mechanical property and corrosion behavior of Ti-3Mo alloy. Corrosion Science, 2022, 200, 110219.	6.6	18
5	Effect of cold deformation on corrosion behavior of selective laser melted 316L stainless steel bipolar plates in a simulated environment for proton exchange membrane fuel cells. Corrosion Science, 2022, 201, 110257.	6.6	46
6	Genes and evolutionary fates of the amanitin biosynthesis pathway in poisonous mushrooms. Proceedings of the National Academy of Sciences of the United States of America, 2022, 119, e2201113119.	7.1	10
7	Hydrogen-assisted failure in partially recrystallized carbon alloyed equiatomic CoCrFeMnNi high-entropy alloy. Corrosion Science, 2022, 203, 110357.	6.6	8
8	Recent advances on environmental corrosion behavior and mechanism of high-entropy alloys. Journal of Materials Science and Technology, 2021, 80, 217-233.	10.7	250
9	Electrochemical migration behavior of moldy printed circuit boards in a 10 mT magnetic field. RSC Advances, 2021, 11, 28178-28188.	3.6	0
10	Differential Expression of Amanitin Biosynthetic Genes and Novel Cyclic Peptides in Amanita molliuscula. Journal of Fungi (Basel, Switzerland), 2021, 7, 384.	3.5	3
11	Hydrogen induced microstructure evolution and cracking mechanism in a metastable dual-phase high-entropy alloy. Materials Science & Engineering A: Structural Materials: Properties, Microstructure and Processing, 2021, 819, 141490.	5.6	19
12	The corrosion behavior and film properties of Al-containing high-entropy alloys in acidic solutions. Applied Surface Science, 2021, 560, 149854.	6.1	58
13	Evolution in microstructure, wear, corrosion, and tribocorrosion behavior of Mo-containing high-entropy alloy coatings fabricated by laser cladding. Corrosion Science, 2021, 191, 109727.	6.6	77
14	Review—Corrosion-Resistant High-Entropy Alloy Coatings: A Review. Journal of the Electrochemical Society, 2021, 168, 111502.	2.9	44
15	X-ray photoelectron spectroscopy and electrochemical investigation of the passive behavior of high-entropy FeCoCrNiMox alloys in sulfuric acid. Applied Surface Science, 2020, 499, 143903.	6.1	89
16	Eigenfrequency characterization and tuning of Ti-6Al-4V ultrasonic horn at high temperatures for glass molding. Ultrasonics, 2020, 101, 106002.	3.9	13
17	Influence of carbon on the corrosion behaviour of interstitial equiatomic CoCrFeMnNi high-entropy alloys in a chlorinated concrete solution. Corrosion Science, 2020, 163, 108287.	6.6	123
18	The passivity of selective laser melted 316L stainless steel. Applied Surface Science, 2020, 504, 144495.	6.1	139

#	Article	IF	CITATIONS
19	Superior resistance to hydrogen damage for selective laser melted 316L stainless steel in a proton exchange membrane fuel cell environment. Corrosion Science, 2020, 166, 108425.	6.6	76
20	Corrosion resistance enhancement of CoCrFeMnNi high-entropy alloy fabricated by additive manufacturing. Corrosion Science, 2020, 177, 108954.	6.6	130
21	A strong and ductile medium-entropy alloy resists hydrogen embrittlement and corrosion. Nature Communications, 2020, 11, 3081.	12.8	116
22	Hydrogen resistance of a 1†GPa strong equiatomic CoCrNi medium entropy alloy. Corrosion Science, 2020, 167, 108510.	6.6	42
23	Mechanism study on microformability of optical glass in ultrasonicâ€assisted molding process. International Journal of Applied Glass Science, 2019, 10, 103-114.	2.0	11
24	Study effects on diamond concentration of CuSnFeNi/diamond composite on grinding WC. International Journal of Advanced Manufacturing Technology, 2019, 104, 2863-2873.	3.0	3
25	Investigation of the Antifouling Mechanism of Electroless Nickel–Phosphorus Coating against Sand and Bitumen. Energy & Fuels, 2019, 33, 6350-6360.	5.1	2
26	Enhancing catalytic activity of tungsten disulfide through topology. Applied Catalysis B: Environmental, 2019, 256, 117802.	20.2	26
27	Effects of Cu particle size on CuSnFeNi/diamond composite processed using hybrid microwave sintering. Powder Metallurgy, 2019, 62, 124-132.	1.7	7
28	A comprehensive study on frictional dependence and predictive accuracy of viscoelastic model for optical glass using compression creep test. Journal of the American Ceramic Society, 2019, 102, 6606-6617.	3.8	17
29	Genome of lethal Lepiota venenata and insights into the evolution of toxin-biosynthetic genes. BMC Genomics, 2019, 20, 198.	2.8	20
30	Reconstruction of high-speed cam curve based on high-order differential interpolation and shape adjustment. Applied Mathematics and Computation, 2019, 356, 272-281.	2.2	9
31	Effects of hydrogen and stress on the electrochemical and passivation behaviour of 304 stainless steel in simulated PEMFC environment. Electrochimica Acta, 2019, 293, 60-77.	5.2	68
32	Corrosion behavior of an equiatomic CoCrFeMnNi high-entropy alloy compared with 304 stainless steel in sulfuric acid solution. Corrosion Science, 2018, 134, 131-139.	6.6	465
33	Characterization of microstructure and properties of electroless duplex Ni-W-P/Ni-P nano-ZrO2 composite coating. Materials Today Physics, 2018, 4, 36-42.	6.0	37
34	Electrochemical and passive behaviour of tin alloyed ferritic stainless steel in concrete environment. Applied Surface Science, 2018, 439, 232-239.	6.1	67
35	Hydrogen embrittlement of an interstitial equimolar high-entropy alloy. Corrosion Science, 2018, 136, 403-408.	6.6	96
36	Zr ₂ N ₂ O Coating-Improved Corrosion Resistance for the Anodic Dissolution Induced by Cathodic Transient Potential. ACS Applied Materials & Interfaces, 2018, 10, 40111-40124.	8.0	19

#	Article	IF	CITATIONS
37	Influence of the aging time on the microstructure and electrochemical behaviour of a 15-5PH ultra-high strength stainless steel. Corrosion Science, 2018, 139, 185-196.	6.6	65
38	Effect of trace Sr and Sc contents and ultrasonic vibration on the microstructure and mechanical properties of the A380 alloy. Advances in Mechanical Engineering, 2018, 10, 168781401877517.	1.6	4
39	Beating hydrogen with its own weapon: Nano-twin gradients enhance embrittlement resistance of a high-entropy alloy. Materials Today, 2018, 21, 1003-1009.	14.2	127
40	Synthesis of a duplex Ni-P-YSZ/Ni-P nanocomposite coating and investigation of its performance. Surface and Coatings Technology, 2017, 311, 70-79.	4.8	44
41	Effects of La2O3 on Mechanical Properties and Corrosion Resistance of H62 Brass. Jom, 2017, 69, 184-190.	1.9	1
42	Anticorrosion performance of chromized coating prepared by pack cementation in simulated solution with H2S and CO2. Applied Surface Science, 2017, 419, 197-205.	6.1	16
43	Hydrogen effects on microstructural evolution and passive film characteristics of a duplex stainless steel. Electrochemistry Communications, 2017, 79, 28-32.	4.7	62
44	Passive Film Properties and Electrochemical Behavior of Co-Cr-Mo Stainless Steel in Chloride Solution. Journal of Materials Engineering and Performance, 2017, 26, 2237-2243.	2.5	9
45	Passivation and electrochemical behavior of 316L stainless steel in chlorinated simulated concrete pore solution. Applied Surface Science, 2017, 400, 38-48.	6.1	171
46	Hydrogen enhances strength and ductility of an equiatomic high-entropy alloy. Scientific Reports, 2017, 7, 9892.	3.3	132
47	Structure-engineered electrocatalyst enables highly active and stable oxygen evolution reaction over layered perovskite LaSr3Co1.5Fe1.5O10-δ. Nano Energy, 2017, 40, 115-121.	16.0	67
48	Effect of cold deformation on the electrochemical behaviour of 304L stainless steel in contaminated sulfuric acid environment. Applied Surface Science, 2017, 425, 628-638.	6.1	70
49	Effect of cold deformation on the corrosion behaviour of UNS S31803 duplex stainless steel in simulated concrete pore solution. Corrosion Science, 2017, 124, 178-192.	6.6	116
50	Influence of pH on the passivation behaviour of 904L stainless steel bipolar plates for proton exchange membrane fuel cells. Journal of Alloys and Compounds, 2016, 686, 216-226.	5.5	52
51	Copper–tungsten electrode wear process and carbon layer characterization in electrical discharge machining. International Journal of Advanced Manufacturing Technology, 2016, 85, 1759-1768.	3.0	12
52	A study on corrosion behaviors of Ni–Cr–Mo laser coating, 316 stainless steel and X70 steel in simulated solutions with H2S and CO2. Surface and Coatings Technology, 2016, 291, 250-257.	4.8	57
53	The passive behaviour of ferritic stainless steel containing alloyed tin in acidic media. RSC Advances, 2016, 6, 9940-9949.	3.6	46
54	Effect of yttrium on properties of copper prepared by powder metallurgy. Advanced Powder Technology, 2015, 26, 1079-1086.	4.1	14

#	Article	IF	CITATIONS
55	The Effect of Melt Overheating on the Melt Structure Transition and Solidified Structures of Al-La Alloy. Jom, 2015, 67, 948-954.	1.9	7
56	Development of electroless Ni–P/nano-WC composite coatings and investigation on its properties. Surface and Coatings Technology, 2015, 277, 99-106.	4.8	115
57	Effects of Melt Thermal-Rate Treatment and Modification of Y on Zn-27Al Alloy. Jom, 2015, 67, 991-995.	1.9	3
58	Electrochemical and passivation behavior investigation of ferritic stainless steel in alkaline environment. Construction and Building Materials, 2015, 96, 502-507.	7.2	67
59	Electrochemical and passivation behavior investigation of ferritic stainless steel in simulated concrete pore media. Data in Brief, 2015, 5, 171-178.	1.0	13
60	Characterization of electrochemical and passive behaviour of Alloy 59 in acid solution. Electrochimica Acta, 2014, 135, 412-419.	5.2	95
61	Sensing application in the precursor region of localized corrosion by scanning electrochemical microscopy. RSC Advances, 2014, 4, 56582-56595.	3.6	7
62	Electrochemical Behavior and Nonlinear Mott-Schottky Characterization of a Stainless Steel Passive Film. Analytical Letters, 2014, 47, 1162-1181.	1.8	29
63	Preparation and characterization of anticorrosion Ormosil sol–gel coatings for aluminum alloy. Journal of Sol-Gel Science and Technology, 2014, 72, 8-20.	2.4	19
64	Scanning electrochemical microscopy study on the electrochemical behavior of CrN film formed on 304 stainless steel by magnetron sputtering. Electrochimica Acta, 2013, 114, 233-241.	5.2	56
65	The electrochemical behaviour of 2205 duplex stainless steel in alkaline solutions with different pH in the presence of chloride. Electrochimica Acta, 2012, 64, 211-220.	5.2	336
66	Electrochemical Behaviour and Surface Analytical of Welded Stainless Steel in the Room Temperature Simulated PWR Water. ISIJ International, 2012, 52, 2266-2272.	1.4	8
67	Characterization of passive film on 2205 duplex stainless steel in sodium thiosulphate solution. Applied Surface Science, 2011, 258, 631-639.	6.1	210